

# Dispersion Energy Enforced Dimerization of a Cyclic Disilylated Plumbylene

Henning Arp, Judith Baumgartner,\* and Christoph Marschner\*

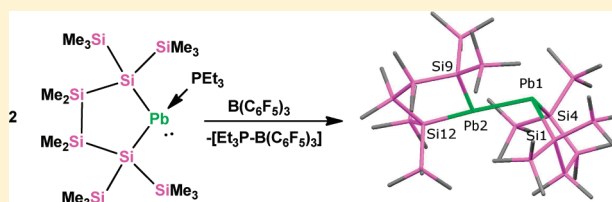
Institut für Anorganische Chemie, Technische Universität Graz, Stremayrgasse 9, A-8010 Graz, Austria

Patrick Zark and Thomas Müller\*

Institut für Reine und Angewandte Chemie, Carl von Ossietzky Universität Oldenburg, Carl von Ossietzky-Str. 9-11, D-26111 Oldenburg, Germany

**S** Supporting Information

**ABSTRACT:** By reaction of 1,4-dipotassio-1,1,4,4-tetrakis(trimethylsilyl)tetramethyltetrasilane with  $\text{PbBr}_2$  in the presence of triethylphosphine a base adduct of a cyclic disilylated plumbylene could be obtained. Phosphine abstraction with  $\text{B}(\text{C}_6\text{F}_5)_3$  led to formation of a base-free plumbylene dimer, which features an unexpected single donor–acceptor  $\text{PbPb}$  bond. The results of density functional computations at the M06-2X and B3LYP level of theory indicate that the dominating interactions which hold the plumbylene subunits together and which define its actual molecular structure are attracting van der Waals forces between the two large and polarizable plumbylene subunits.



## INTRODUCTION

The isolation of the first stable germylenes and stannylenes was accomplished by Lappert and co-workers<sup>1,2</sup> approximately 35 years ago, and still the chemistry of these heavier carbene analogues continues to attract the attention of both experimentally and theoretically oriented chemists.<sup>3,4</sup>

One major reason for this interest is the fundamental differences in electronic ground states, structures, and reactivities between carbenes and their dimers, i.e. alkenes, and their heavier counterparts the metallylenes and dimetallylenes. Heavy metallylenes exhibit singlet ground states with an increasing singlet–triplet gap with rising atomic number.<sup>5</sup> This is caused by the increasing energy difference between their *s*- and *p*-orbital levels and the consequential lack of orbital mixing. However, by attaching large electropositive substituents to the divalent group 14 atom to some extent they can be forced into mixing their *s*- and *p*-orbitals and thus significantly lower the singlet–triplet gap. This behavior is illustrated by Sekiguchi's distannene ( ${}^t\text{Bu}_2\text{MeSi}$ )<sub>2</sub>Sn=Sn(SiMe<sup>t</sup>Bu<sub>2</sub>)<sub>2</sub> that despite bearing bulky groups on the tin atoms does not dissociate into monomers in solution.<sup>6</sup>

The tendency to form monomeric compounds is even more pronounced on descending group 14 to lead. This is well exemplified by the difference between bis[tris(trimethylsilyl)silyl]tin and -lead.<sup>7</sup> Both compounds exist as monomers in solution, but the tin compound crystallizes as a distannene type dimer while the lead compound retains the monomeric plumbylene structure in the solid state.<sup>7,8</sup> After our recent synthesis<sup>9</sup> of a bicyclic distannene, utilizing the dimerization of

a bidentate oligosilanylene ligated stannylene, we wanted to extend this study to lead.

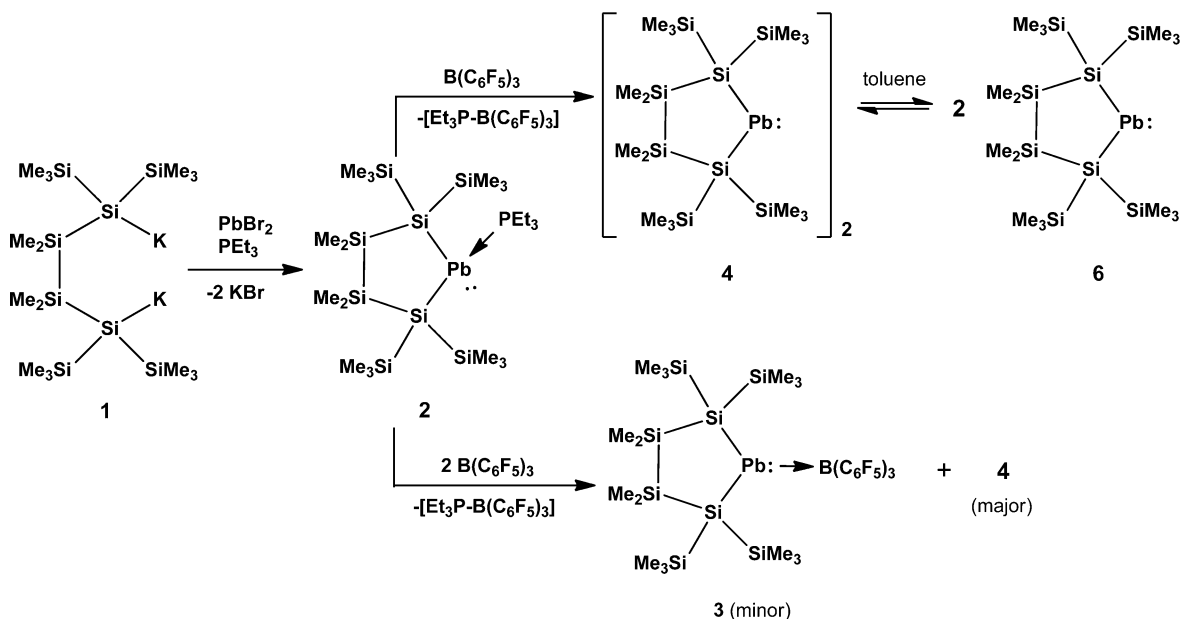
## RESULTS AND DISCUSSION

**Synthesis.** The synthesis of the plumbylene phosphine adduct **2** was accomplished by addition of 1,4-dipotassio-tetrasilane **1**<sup>10,11</sup> to a suspension of  $\text{PbBr}_2$  and  $\text{PEt}_3$  (Scheme 1). Generation of the “base free” plumbylene dimer **4** could then be achieved by abstraction of triethylphosphine from **2** with the strong Lewis acid  $\text{B}(\text{C}_6\text{F}_5)_3$  (Scheme 1). The thus formed phosphine adduct of the borane<sup>12</sup> could be separated by fractional crystallization, but nevertheless several attempts of recrystallization from pentane were required to grow crystals of plumbylene dimer **4** suitable for X-ray diffraction (XRD). On one occasion together with much amorphous black material (shown by NMR spectroscopy to be **4**) a few green symmetrically shaped crystals were found. By X-ray crystal structure analysis these were found to correspond to the plumbylene- $\text{B}(\text{C}_6\text{F}_5)_3$  adduct **3** (Figure 2). However, even when 2 equiv of  $\text{B}(\text{C}_6\text{F}_5)_3$  were used in the reaction with **2** only trace amounts of **3** below the NMR detection limit were formed. This behavior toward  $\text{B}(\text{C}_6\text{F}_5)_3$  differs from our recently published results of the same reaction sequence applied to the corresponding stannylene phosphine adduct.<sup>9</sup> In the tin case the stannylene borane adduct could be formed selectively suppressing a competing dimerization process. The dimeric structure of compound **4** was proven by XRD (Figure

Received: January 20, 2012

Published: March 28, 2012

Scheme 1. Synthesis of Plumbylene Adducts 2 and 3 and Plumbylene Dimer 4 Which Dissociates to Plumbylene 6 in Solution



3). While the phosphine complex 2 was found to be infinitely stable in solution as well as in the solid state under exclusion of moisture and air, plumbylene dimer 4 decomposed in solution at room temperature to elemental lead and the corresponding cyclotetrasilane, resulting from the reductive elimination of lead.

**NMR Spectroscopy.** For plumbylene phosphine adduct 2 at rt, no  $^{207}\text{Pb}$  NMR signal could be detected. This is probably due to a dissociation–association process of the phosphine. This is also indicated by the  $^{31}\text{P}$  NMR spectrum, where a broad signal at  $\delta = -60.0$  ppm without resolved coupling to  $^{207}\text{Pb}$  is observed. In the  $^{29}\text{Si}$  NMR spectrum sharp signals for the  $\text{SiMe}_2$  units at  $\delta = -10.7$  and the quaternary silicon atoms at  $\delta = -87.3$  ppm were found as expected while the  $\text{SiMe}_3$  resonances appeared as a badly resolved broad signal at  $\delta = -1.5$  ppm. This can also be rationalized by the said dissociation–association process of the phosphine. In the  $^1\text{H}$  and  $^{13}\text{C}$  NMR spectra the expected pattern of signals was found. Cooling to  $-60$  °C allows the observation of a  $^{207}\text{Pb}$  resonance at  $\delta = +1139$  ppm as a doublet with a coupling constant of  $^1J_{(\text{PbP})} = 3083$  Hz which was also observed in the  $^{31}\text{P}$  NMR spectrum at the same temperature. This chemical shift agrees fairly well with an expected value of  $\delta = +1595$  ppm based on Wrackmeyer's empirical correlation<sup>13</sup> of NMR chemical shifts of Sn(II) compounds to analogous Pb(II) compounds.<sup>13</sup>

For the plumbylene dimer 4 again no  $^{207}\text{Pb}$  NMR signals could be observed at rt, as decomposition of 4 in solution proved to be faster than acquisition of the  $^{207}\text{Pb}$  NMR spectrum. The decomposition takes place in an analogous way to bis[tris(trimethylsilyl)silyl]lead (5),<sup>7</sup> but with a shorter lifetime. After 30 min in a benzene solution, complete decomposition to 1,1,2,2-tetrakis(trimethylsilyl)-tetramethylcyclotetrasilane<sup>14</sup> and elemental lead occurred. Nevertheless, acquisition of spectra at  $-40$  °C allowed observation of a  $^{207}\text{Pb}$  resonance with a chemical shift of  $\delta = +19516$  ppm, which to the best of our knowledge is by far the most downfield shifted resonance of a lead compound ever recorded. This strong paramagnetically deshielded resonance is

typical for tetrylenes which have small energy separations between occupied and virtual molecular orbitals with large coefficients at the magnetic active nuclei.<sup>15</sup> Furthermore, the strongly deshielded  $^{207}\text{Pb}$  NMR signal clearly indicates that dimer 4 exists as plumbylene monomer, 6, in solution (see Scheme 1). When the  $^{207}\text{Pb}$  shifts of related plumbylenes such as  $\text{PbAr}^*[\text{Si}(\text{SiMe}_3)_3]$  ( $\text{Ar}^* = \text{C}_6\text{H}_3\text{-2,6-Me}_2$ ) ( $\delta = +10510$  ppm)<sup>16</sup> and  $\text{Pb}\{(\text{Me}_3\text{Si})_2(\text{CSiMe}_2\text{CH}_2)\}_2$  ( $\delta = +10050$  ppm) are considered,<sup>17</sup> a chemical shift of this order of magnitude seems reasonable. With respect to the  $^{29}\text{Si}$  chemical shift for the silicon atom attached to lead Klinkhammer and co-workers reported resonances of  $\delta = +198.6$  for  $\text{Pb}[\text{Si}(\text{SiMe}_3)_3]_2$ <sup>7,16</sup> and  $\delta = +156.5$  for  $\text{PbAr}^*[\text{Si}(\text{SiMe}_3)_3]$ .<sup>16</sup> However, we did not find any signal in this area. Comparison with the  $^{29}\text{Si}$  NMR chemical shifts of related stannylene derivatives<sup>18</sup> suggests a  $^{29}\text{Si}$  NMR chemical shift for this silicon atom in plumbylene 6 close to  $\delta = 0$  ppm. This assumption was further supported by theoretical investigations, which predict for the  $\alpha$ -silicon atom in plumbylene 6 a chemical shift of  $\delta = -35$  ppm.<sup>19</sup> Our measurement at  $-40$  °C eventually led to the observation of a signal at  $\delta = -8.5$  ppm which we tentatively assign to the  $\alpha$ -Si resonance.

**X-ray Crystallography.** Compounds 2, 3, and 4 were subjected to single-crystal X-ray diffraction analysis, and the structural features are listed in Table S1. The structure of 2 (Figure 1) is the first plumba-cyclopentasilane to be structurally characterized. Similar to the recently published cyclopentasilanyl stannylene phosphine adduct<sup>9</sup> it adopts an envelope conformation with one of the quaternary Si atoms on the flap. The donor–acceptor interaction with the phosphine is clearly indicated by the strong pyramidalization of the Pb atom in 2 [pyramidalization angle  $\beta(\text{Pb}) = 71.2^\circ$ ]<sup>20</sup> and by the Pb–P bond (274.0 pm) which is significantly longer than the sum of the covalent radii (255 pm).<sup>21</sup>

The plumbylene borane adduct 3 (Figure 2) is an analogue to the stannylene borane adduct reported by us earlier.<sup>9</sup> The lead atom in compound 3 is in an approximate trigonal planar coordination environment with only a small deviation from planarity [ $\beta(\text{Pb}) = 7.9^\circ$ ] and a relatively long B–Pb bond

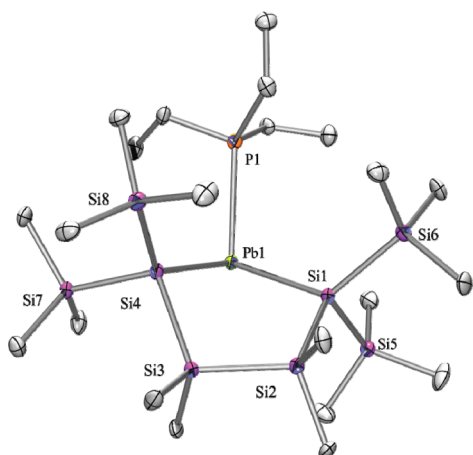


**Figure 1.** Molecular structure of **2** (thermal ellipsoid plot drawn at the 30% probability level). Hydrogen atoms omitted for clarity (bond lengths in pm, angles in deg). Pb(1)–Si(4) 272.3(2), Pb(1)–Si(1) 272.8(2), Pb(1)–P(1) 274.0(2), Si(1)–Si(2) 237.1(3), P(1)–C(19) 182.9(10), Si(2)–C(2) 189.8(9), Si(4)–Pb(1)–Si(1) 95.67(8), Si(4)–Pb(1)–P(1) 97.86(7), Si(1)–Pb(1)–P(1) 106.01(7).

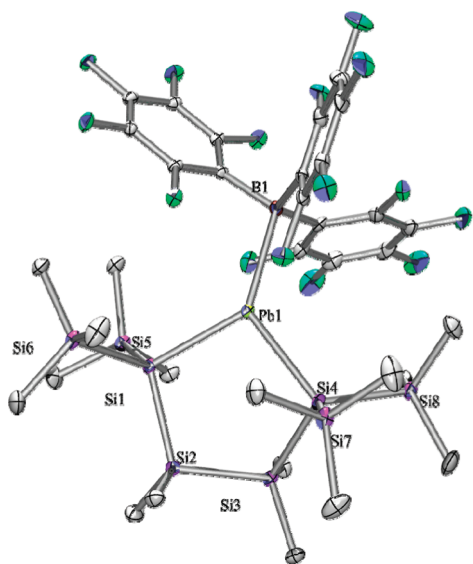


**Figure 2.** Molecular structure of **3** (thermal ellipsoid plot drawn at the 30% probability level). Hydrogen atoms omitted for clarity (bond lengths in pm, angles in deg). Pb(1)–B(1) 243.4(7), Pb(1)–Si(1) 266.54(17), Pb(1)–Si(4) 266.91(18), B(1)–Pb(1)–Si(1) 131.06(16), B(1)–Pb(1)–Si(4) 125.26(16), Si(1)–Pb(1)–Si(4) 102.80(6).

[243.5 pm (**3**) vs 229 pm (sum of the covalent radii)].<sup>21</sup> Both features are in agreement with the predominant plumblylene/borane donor/acceptor interaction. In addition, the plumblylene is also acting as a Lewis acid by accepting electron donation from one of the *ortho*-fluorines of the  $\text{BAR}_f$  moiety. This is indicated in the solid state by a relative close  $\text{F}\cdots\text{Pb}$  contact of 277.8 pm, halfway between the sum of the covalent and van der Waals radii (208 and 349 pm).<sup>21,22</sup>

In contrast to Klinkhammer's disilylated monomeric plumblylene ( $[(\text{Me}_3\text{Si})_3\text{Si}]_2\text{Pb}$ ) (**5**) the crystal structure analysis of **4** (Figure 3) revealed a dimeric arrangement with a Pb–Pb separation of 306.4 pm. This is substantially longer than a typical Pb–Pb single bond of 284 pm such as found for hexaphenyldiplumbane,<sup>23</sup> but well within the range of 284–354

pm covered by Klinkhammer's heteroleptic plumblylene dimers of the type  $\{[(\text{Me}_3\text{Si})_3\text{Si}]\text{ArPb}\}_2$ .<sup>8</sup> The two plumblylene units of **4** show different arrangements around the lead atoms. The Pb(1) atom in Figure 3 shows some stereochemical activity of

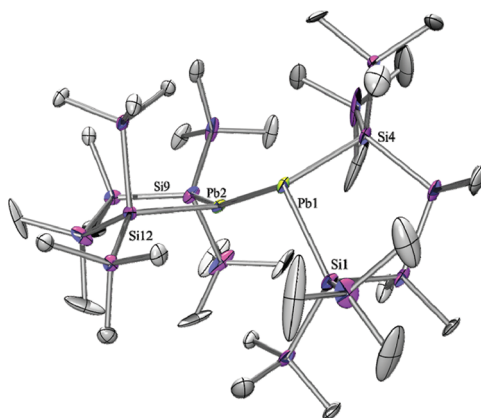


**Figure 3.** Molecular structure of **4** (thermal ellipsoid plot drawn at the 30% probability level). Hydrogen atoms omitted for clarity (bond lengths in pm, angles in deg). Pb(1)–Si(4) 270.9(4), Pb(1)–Si(1) 273.2(3), Pb(1)–Pb(2) 306.40(8), Pb(2)–Si(12) 269.7(3), Pb(2)–Si(9) 273.7(3), Si(1)–Si(2) 233.4(6), Si(2)–C(1) 187.5(13), Si(4)–Pb(1)–Si(1) 94.38(12), Si(4)–Pb(1)–Pb(2) 109.54(11), Si(1)–Pb(1)–Pb(2) 101.83(7), Si(12)–Pb(2)–Si(9) 96.49(10), Si(12)–Pb(2)–Pb(1) 101.80(7), Si(9)–Pb(2)–Pb(1) 156.09(9).

the lone pair, and it is therefore highly pyramidalized with both  $\text{SiPb(1)Pb(2)}$  bond angles being close to the tetrahedral angle of  $109.5^\circ$  and a pyramidalization angle  $\beta(\text{Pb(1)}) = 66.0^\circ$ .<sup>20</sup> Pb(2) to the contrary shows a distorted planar geometry, the sum of bond angles around Pb(2) being  $354.3^\circ$  concomitant by a pyramidalization angle  $\beta$  of  $15.1^\circ$ . This very unusual structural arrangement can be rationalized by assuming a single donor–acceptor interaction in the solid state between the two plumblylene units with the planar Pb(2) being the donor and the pyramidalized Pb(1) acting as the acceptor. A somewhat similar situation is found in distannene  $(\text{Me}_2\text{PbSn})_2$  ( $\text{Me}_{\text{bp}} = 2,3,4\text{-methyl-6-tert-butylphenyl}$ )<sup>24</sup> and, in particular, in Weidenbruch's cyclotriplumbane  $(\text{Tep}_2\text{Pb})_3$  ( $\text{Tep} = 2,4,6\text{-triethylphenyl}$ ), where each lead atom acts as an electron pair acceptor for one of its neighbors and as a donor to the other one.<sup>25</sup> As the geometry of the core in Weidenbruch's compounds depends on subtle changes in the steric bulk of the ligands, plumblylene **6** might adopt an intermediate position.<sup>25–27</sup> The electronic situation would favor trimerization, while the silyl ligands employed do not allow higher aggregates than a dimer for steric reasons.

**Computational Study.** Quantum mechanical calculations at the M06-2X/SDD(Pb) 6-31G(d)(P, Si, F, C, B, H) level, here denoted as M06-2X/A, provided a more detailed picture of the bonding in **4**, the dimeric form of plumblylene **6**, and the related plumblylene complexes with  $\text{PET}_3$  (**2**) and  $\text{B}(\text{C}_6\text{F}_5)_3$  (**3**).<sup>28,29</sup> The molecular structures, which were predicted by the calculations for compounds **2–4**, are in good qualitative agreement with the data obtained from XRD measurements (Figure 4). In addition, the results of the calculations reveal for the free plumblylene **6** a half-chair conformation of the plumbacyclopentasilane ring with an endocyclic  $\text{SiPbSi}$  bond angle  $\alpha = 90.5^\circ$  and  $\text{Pb(II)Si(IV)}$  bonds which are by 4–5 pm longer than reported for Pb–Si linkages in other plumblylenes (Figure 4).<sup>30</sup> The substitution with the electropositive silyl

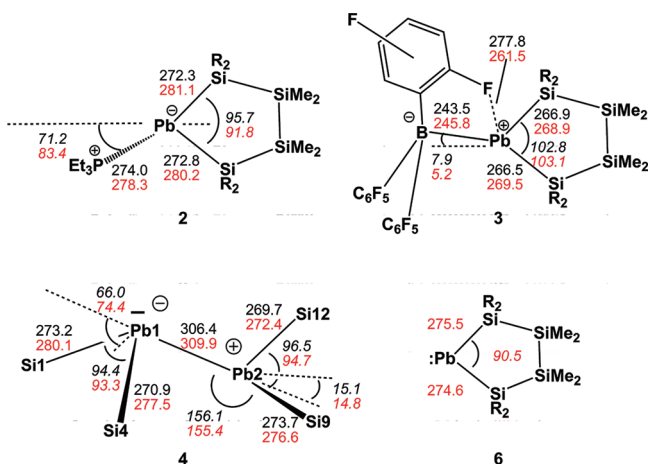


**Figure 4.** Comparison between experimental (XRD, black) and calculated [M06-2X/A, red] structural parameter of compounds 2, 3, the central part of dimer 4 and computed structural data of 6. Bond angles  $\alpha$  and pyramidalization angles  $\beta$  in deg (italic), bond lengths in pm ( $R = \text{SiMe}_3$ ).

groups decreases markedly the computed singlet–triplet energy difference,  $\Delta E(\text{ST})$ , for tetrylene 6 compared to the parent plumbylene  $\text{PbH}_2$  [ $\Delta E(\text{ST}) = -215.4 \text{ kJ mol}^{-1}$  ( $\text{PbH}_2$ ),  $\Delta E(\text{ST}) = -145.4 \text{ kJ mol}^{-1}$  (6)]. Due to the small endocyclic SiPbSi bond angle  $\alpha$ ,  $\Delta E(\text{ST})$  is however larger than that predicted for Klinkhammer’s plumbylene 5 [ $\Delta E(\text{ST}) = -128.9 \text{ kJ mol}^{-1}$  (5)]. According to an NBO analysis<sup>29</sup> the donor–acceptor interaction between plumbylene 6 and the phosphine molecule in complex 2 is accompanied by an electron transfer of 0.25 au from the phosphine to the plumbylene and results in a calculated donor–acceptor bond strength BE of  $-76.0 \text{ kJ mol}^{-1}$ .<sup>29,31</sup> Both distinct features which are found in the experimental solid state structure of the plumbylene/borane

Lewis base/acid complex 3, the almost trigonal planar coordination of the Pb atom and the close contact between the *ortho*-fluorine and the Pb-atom, are also present in the calculated gas phase structure of 3. This finding excludes the possibility that the close F...Pb contact found in the solid state structure is a consequence of crystal packing effects, and it suggests the presence of a structure shaping C–F  $\rightarrow$  Pb donor–acceptor interaction. The results of the NBO analysis reveal an overall electron donation from the plumbylene to the borane in 3 of 0.95 au, and the donor–acceptor bond strength BE of the Pb–B bond is calculated to be  $-65.1 \text{ kJ mol}^{-1}$ .<sup>29,31</sup>

According to the results of the computations the overall molecular structure of the plumbicyclopentasilane ring of plumbylene 6 is conserved nearly unchanged in the acceptor complex 2 and in the donor adduct 3 and also in the plumbylene dimer 4. In agreement with the experimental data Pb atoms with two significantly different coordination environments were found in the computed structure of dimer 4 (Figures 3 and 4). The structural data suggest a single donor–acceptor interaction between the plumbylene subunits with a distorted trigonal planar Pb(2) atom ( $\beta(\text{Pb}(2)) = 14.8^\circ$ ),<sup>20</sup> acting as the donor and a strongly pyramidalized second Pb(1) atom ( $\beta(\text{Pb}(1)) = 74.4^\circ$ )<sup>20</sup> (see Figures 4, 5). This interaction results in a relative long Pb(2)Pb(1) bond ( $d(\text{Pb}(1)\text{Pb}(2)) = 309.9 \text{ pm}$ ). The conformation around this bond with a dihedral angle of  $74.5^\circ$  between the planes spanned by the Pb atoms and their adjacent Si atoms excludes a second donor–acceptor interaction (Figure 5a). Consequently, the frontier orbitals of dimer 4 are the stereochemically active electron pair at Pb(1) (HOMO) and the vacant p-type orbital at Pb(2) (LUMO) (Figure 5b). The NBO analysis suggests a significant electron transfer from the donor plumbylene to the acceptor plumbylene of 0.24 au which results in a calculated Wiberg bond index (WBI) for the donor–acceptor bond in dimer 4 of

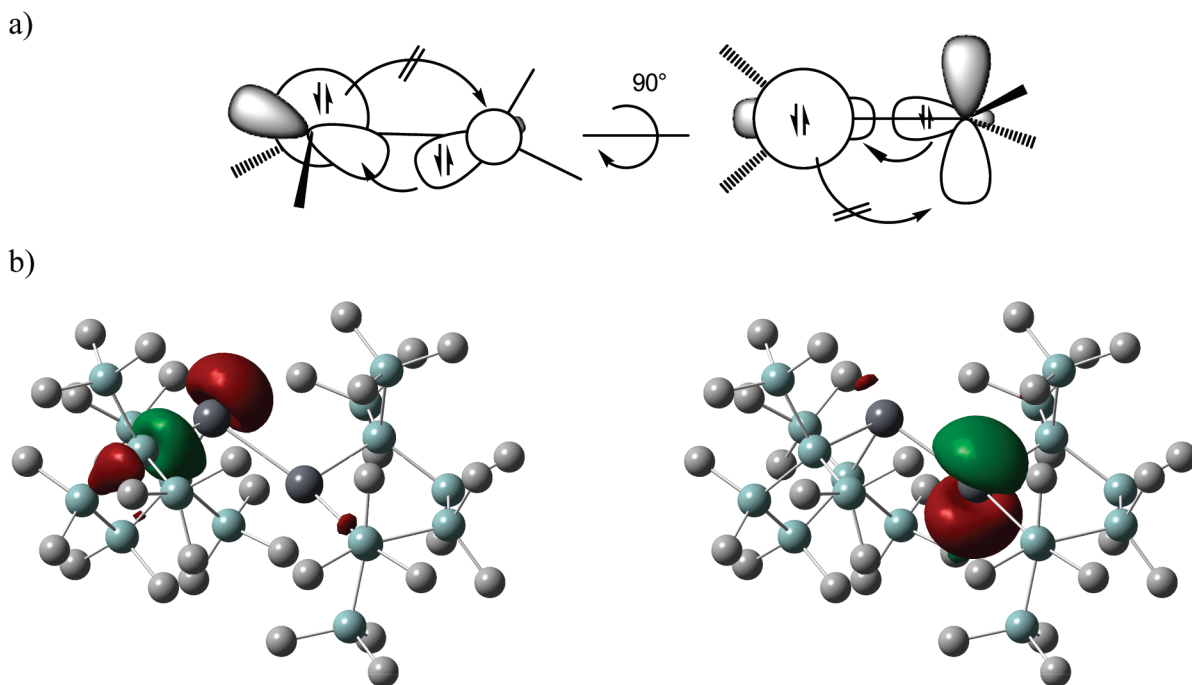
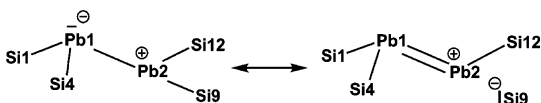


**Figure 5.** (a) Schematic view of the donor–acceptor bond in plumbylene dimer 4. Left: View in the direction orthogonal to the Pb(2)Si(9)Si(12) plane. Right: After rotation by  $90^\circ$  around the Pb(1)Pb(2) bond. (b) Calculated surface diagrams of HOMO (left) and LUMO (right) of dimer 4 (isodensity value: 0.05; color code: dark gray: Pb; blue gray: Si; light gray: C; H-atoms omitted).



0.70. This value is smaller than those computed for the Pb–Pb single bond in staggered  $\text{Pb}_2\text{H}_6$  [point group (PG):  $D_{3d}$ ,  $d(\text{PbPb}) = 288.8$  pm, WBI = 0.88] and in trans bent  $\text{Pb}_2\text{H}_4$  [PG:  $C_{2h}$ ,  $d(\text{PbPb}) = 290.9$  pm, WBI = 0.87]. According to the NBO analysis the Pb–Pb linkage in dimer 4 is supported by negative hyperconjugation which involves the lone pair at Pb(1) and the  $\sigma^*$  orbital of the Pb(2)–Si(9) bond (see Scheme 2). As a result from this interaction the bond angle  $\alpha(\text{Pb}(1),$

**Scheme 2. Canonical Structures Which Describe the Negative Hyperconjugation in Dimer 4**



$\text{Pb}(2)\text{Si}(9)$  is significantly widened [ $\alpha(\text{Pb}(1)\text{Pb}(2)\text{Si}(9)) = 155.4^\circ$ ] and the  $\text{Pb}(2)\text{Si}(9)$  (276.6 pm) bond is longer than the comparable  $\text{Pb}(2)\text{Si}(12)$  bond (272.4 pm). Consequently, also the computed WBIs of these two bonds differ markedly [WBI ( $\text{Pb}(2)\text{Si}(9)$ ) = 0.64] and WBI ( $\text{Pb}(2)\text{Si}(12)$ ) = 0.71].<sup>32</sup>

The overall binding energy BE between both plumblylene subunits in dimer 4 is computed to be  $-110.8$   $\text{kJ mol}^{-1}$ .<sup>31,33</sup> Therefore, the PbPb linkage in 4 is considerably stronger than the PbPb bond in the parent diplumbene  $\text{Pb}_2\text{H}_4$  in its trans bent conformation [ $\text{BE}(\text{Pb}_2\text{H}_4) = -62.4$   $\text{kJ mol}^{-1}$ ], although on the basis of the computed WBIs (see above) a stronger PbPb bond in  $\text{Pb}_2\text{H}_4$  is expected. In addition, on the basis of the computed singlet/triplet separations  $E(\text{ST})$  for plumblylenes 5 and 6 (see above) and the nonexistence of a dimer of plumblylene 5, the formation of dimer 4 is completely unexpected. This suggests that it is not the conventional donor–acceptor bonding interaction that ties both plumblylene subunits in dimer 4 together. A qualitative assessment of the attractive coulomb potential,  $E_C$ , between the two Pb-atoms which results from charge transfer between both plumblylene subunits indicates that this factor is of only minor importance as it accounts for less than 25% of the computed BE ( $E_C = -25.8$   $\text{kJ mol}^{-1}$ ).<sup>34</sup> This leaves the attractive dispersion potential between the large and polarizable substituents of plumblylene 6 as the decisive force for an understanding of the bonding situation. A related situation is found in the sterically overloaded disilane  ${}^t\text{Bu}_3\text{Si}-\text{Si}{}^t\text{Bu}_3$  which is marked by an extremely long Si–Si bond but shows a comparatively high thermostability.<sup>35,36</sup> Recently, dispersion forces were also recognized as important factors that explain the high stability of organometallic compounds<sup>37</sup> and that of hydrocarbons with extremely long alkane C–C bonds.<sup>38</sup> The here applied M06-2X functional properly accounts for noncovalent van der Waals interactions, while the most prominent deficit of the popular B3LYP functional is the nearly complete negligence of dispersion.<sup>39</sup> Therefore, the difference in the calculated bond energies using these two functionals allows estimating the contribution of noncovalent bonding in dimer 4.<sup>37,38</sup> As expected for the parent  $\text{Pb}_2\text{H}_4$  nearly the same Pb–Pb bond energy BE is computed using the two different functionals [M06-2X/A//M06-2X/A:  $\text{BE}(\text{Pb}_2\text{H}_4) = -62.4$   $\text{kJ mol}^{-1}$ ; B3LYP/A//M06-2X/A:  $\text{BE}(\text{Pb}_2\text{H}_4) = -54.4$   $\text{kJ mol}^{-1}$ ]<sup>29</sup> indicating that attracting dispersion forces are not significant. In sharp contrast in the case of dimer 4 dispersion forces are decisive as the B3LYP functional predicts an even positive Pb–Pb bond energy BE [M06-2X/A//M06-2X/A:  $\text{BE}(4) = -110.8$   $\text{kJ mol}^{-1}$ ; B3LYP/A//M06-2X/A:  $\text{BE}(4) = +1.0$   $\text{kJ mol}^{-1}$ ]. In

addition free optimization of the molecular structure of dimer 4 using the B3LYP/A method results in a Pb(1)–Pb(2) bond, which is by 19.7 pm longer than determined by XRD. Furthermore, the computed binding energy BE for the free optimized dimer 4 at B3LYP/A is considerably decreased compared to the M06-2X value [B3LYP/A//B3LYP/A:  $\text{BE}(4) = -26.5$   $\text{kJ mol}^{-1}$ ].

A rotational isomer of dimer 4, the diplumblylene 7, with an approximate *trans* bent configuration of the constituent plumblylenes 6 and a slightly smaller Pb–Pb separation was located on the potential energy surface [Pb–Pb = 298.2 pm,  $\beta(\text{Pb}) = 52.2^\circ$  and  $36.9^\circ$ ]. In this conformer both plumblylenes are connected by a conventional double donor–acceptor interaction. The binding energy for *trans* bent dimer 7 is however significantly smaller than calculated for dimer 4 [BE =  $-76.4$   $\text{kJ mol}^{-1}$  (7) vs  $-110.8$   $\text{kJ mol}^{-1}$  (4) at M06-2X/A]. Interestingly, B3LYP computations applied at both plumblylene dimers at their M06-2X equilibrium structures predict both dimers to be nearly equal in energy with dimer 7 being slightly more stable by 0.5  $\text{kJ mol}^{-1}$ . The results of these model calculations suggest that it is solely the optimization of the dispersion energy as interplay between attracting and repelling forces between the plumblylene subunits which determines the actual shape of the plumblylene dimer 4.

The analysis of the computational results indicates that the dominant attracting force that holds together dimer 4 in its inmost folds<sup>40</sup> is van der Waals interaction, which is supported by a comparatively weak donor–acceptor interaction. In addition, it is the stronger dispersion energy contribution that prefers the single donor–acceptor dimer 4 over the *trans* bent dimer 7 with an double donor–acceptor interaction between the constituent plumblylenes. At this stage of the discussion we feel that it is appropriate to point out that in the past many elaborate analyses of bonding in organometallic compounds,<sup>41</sup> in particular in systems with important donor–acceptor interactions, the contributions of the attractive dispersion interactions between the experimentally often unavoidable large substituents are neglected although they might be decisive. This realization calls for a computational reinvestigation of these systems.

## EXPERIMENTAL SECTION

**General Remarks.** All reactions involving air-sensitive compounds were carried out under an atmosphere of dry nitrogen or argon using either Schlenk techniques or a glovebox. All solvents were dried using a column based solvent purification system.<sup>42</sup> Potassium *tert*-butanolate was purchased from Merck. All other chemicals were obtained from different suppliers and used without further purification.

<sup>1</sup>H (300 MHz), <sup>13</sup>C (75.4 MHz), <sup>31</sup>P (124.4 MHz), <sup>207</sup>Pb (62.8 MHz), and <sup>29</sup>Si (59.3 MHz) NMR spectra were recorded on a Varian INOVA 300 spectrometer. For all samples  $\text{C}_6\text{D}_6$  was used as solvent if not stated otherwise. To compensate for the low isotopic abundance of <sup>29</sup>Si the INEPT pulse sequence<sup>43,44</sup> was used for the amplification of the signal.

**X-ray Structure Determination.** For X-ray structure analyses the crystals were mounted onto the tip of glass fibers, and data collection was performed with a BRUKER-AXS SMART APEX CCD diffractometer using graphite-monochromated Mo  $K\alpha$  radiation (0.71073 Å). The data were reduced to  $F^2$  and corrected for absorption effects with SAINT<sup>45</sup> and SADABS,<sup>46,47</sup> respectively. The structures were solved by direct methods and refined by the full-matrix least-squares method (SHELXL97).<sup>48</sup> If not noted otherwise all non-hydrogen atoms were refined with anisotropic displacement parameters. All hydrogen atoms were located in calculated positions to correspond to standard bond lengths and angles. All diagrams were

drawn with 30% probability thermal ellipsoids, and all hydrogen atoms were omitted for clarity.

Crystallographic data (excluding structure factors) for the structures of compounds **2**, **3**, and **4** reported in this paper have been deposited with the Cambridge Crystallographic Data Center as supplementary publication no. CCDC-831746 (**2**), 831750 (**3**), and 831749 (**4**). Copies of data can be obtained free of charge at <http://www.ccdc.cam.ac.uk/products/csd/request/>.

1,1,1,4,4,4-Hexakis(trimethylsilyl)tetramethyltetrasilane<sup>11</sup> and B(C<sub>6</sub>F<sub>5</sub>)<sub>3</sub><sup>49</sup> were prepared according to literature procedures.

**Plumbylene Phosphine Adduct 2.** After stirring a solution of 1,1,1,4,4,4-hexakis(trimethylsilyl)tetramethyltetrasilane (612 mg, 1.0 mmol) and KO<sup>t</sup>Bu (236 mg, 2.1 mmol) in THF (5 mL) for 18 h at 60 °C the solution was cooled to rt and added dropwise to a stirred suspension of PbBr<sub>2</sub> (367 mg, 1.0 mmol) and PEt<sub>3</sub> (120 mg, 1.0 mmol) in THF (5 mL). On addition a color change from green to red appeared, and the resulting red suspension was stirred for 2 h. All volatiles were removed under reduced pressure, and the residue was extracted three times with pentane (5 mL each). The red solution was concentrated to 4 mL and stored at -60 °C for 36 h. Red crystals of **2** (569 mg, 72%) were isolated by filtration and dried in vacuo. <sup>1</sup>H NMR (δ in ppm): 1.24 (pseudo quintet, J(apparent): 7.5 Hz, 6H, P(CH<sub>2</sub>CH<sub>3</sub>)<sub>3</sub>), 0.59 (td, <sup>3</sup>J<sub>HH</sub> = 7.6 Hz, <sup>3</sup>J<sub>PH</sub> = 15.1 Hz, P(CH<sub>2</sub>CH<sub>3</sub>)<sub>3</sub>), 0.50 (s, 12 H, SiMe<sub>2</sub>), 0.46 (s, 36H, SiMe<sub>3</sub>). <sup>13</sup>C NMR (δ in ppm): 19.6 (d, <sup>2</sup>J<sub>PC</sub> = 4.5 Hz, P(CH<sub>2</sub>CH<sub>3</sub>)<sub>3</sub>), 9.9 (s, P(CH<sub>2</sub>CH<sub>3</sub>)<sub>3</sub>), 5.1 (SiMe<sub>3</sub>), 2.3 (SiMe<sub>2</sub>). <sup>29</sup>Si NMR (δ in ppm): -1.7 (br, SiMe<sub>3</sub>), -10.7 (SiMe<sub>2</sub>), -87.3 (quart. Si). <sup>31</sup>P NMR (δ in ppm): -60.0 (br, PEt<sub>3</sub>); (solution in THF-d<sub>8</sub>, -60 °C): -53.9 (d, <sup>1</sup>J<sub>PbP</sub> = 3087 Hz). <sup>207</sup>Pb NMR (δ in ppm, solution in THF-d<sub>8</sub>, -60 °C): 1139 (d, <sup>1</sup>J<sub>PbP</sub> = 3083 Hz); no signal at rt.

**Plumbylene Dimer 4.** A mixture of **2** (100 mg, 0.13 mmol) and B(C<sub>6</sub>F<sub>5</sub>)<sub>3</sub> (67 mg, 0.13 mmol) was dissolved in pentane (10 mL) and stirred for 5 min. The color changed from red to black during this period. The dark reaction mixture was centrifuged and stored at -30 °C for 12 h. Colorless (C<sub>6</sub>F<sub>5</sub>)<sub>3</sub>B-PEt<sub>3</sub> was removed by filtration at -30 °C. The remaining black solution was concentrated to 5 mL and stored at -60 °C for 24 h. The obtained material contained small impurities of **3**. Compound **4** (84 mg, 96%) was isolated after several recrystallization steps with pentane as black plates. NMR data for the monomeric plumbylene **6**: <sup>1</sup>H NMR (δ in ppm, rt): 0.47 (s, 12H, SiMe<sub>2</sub>), 0.24 (s, 36H, SiMe<sub>3</sub>); (solution in toluene-d<sub>8</sub>, -40 °C): 0.62 (s, 12H, SiMe<sub>2</sub>), 0.42 (s, 36H, SiMe<sub>3</sub>). <sup>13</sup>C: (δ in ppm, solution in toluene-d<sub>8</sub>, -40 °C): 6.4 (SiMe<sub>3</sub>), 5.0 (SiMe<sub>2</sub>). <sup>29</sup>Si (δ in ppm, solution in toluene-d<sub>8</sub>, -40 °C): 3.2 (SiMe<sub>2</sub>), 1.5 (SiMe<sub>3</sub>), -8.5 (PbSi). <sup>207</sup>Pb (δ in ppm, solution in toluene-d<sub>8</sub>, -40 °C): 19516; no signal at rt.

## ■ ASSOCIATED CONTENT

### Ⓢ Supporting Information

Details for the calculated structures of compounds **2**–**7**, as well as X-ray crystallographic information for compounds **2**, **3**, and **4** in CIF format. This material is available free of charge via the Internet at <http://pubs.acs.org>.

## ■ AUTHOR INFORMATION

### Corresponding Authors

baumgartner@tugraz.at;  
christoph.marschner@tugraz.at;  
thomas.mueller@uni-oldenburg.de.

### Notes

The authors declare no competing financial interest.

## ■ ACKNOWLEDGMENTS

This work is dedicated to Prof. Akira Sekiguchi on the occasion of his 60th birthday. Support of the study was provided by the Austrian *Fonds zur Förderung der Wissenschaften* (FWF) via the project P-21346 (J.B.). P. Zark thanks the *Fonds der Chemischen*

*Industrie* (FCI) for a scholarship (No.183191) and the High-Performance Computing centre of CvO university is thanked for computer time.

## ■ REFERENCES

- (1) Goldberg, D. E.; Harris, D. H.; Lappert, M. F.; Thomas, K. M. *J. Chem. Soc., Chem. Commun.* **1976**, 261–262.
- (2) Goldberg, D. E.; Hitchcock, P. B.; Lappert, M. F.; Thomas, K. M.; Thorne, A. J.; Fjeldberg, T.; Haaland, A.; Schilling, B. E. R. *J. Chem. Soc., Dalton Trans.* **1986**, 2387–2394.
- (3) Ganzer, I.; Hartmann, M.; Frenking, G. In *The Chemistry of Organic Germanium, Tin and Lead Compounds Vol. 2*; Rappoport, Z., Ed.; John Wiley & Sons, Ltd.: 2002; pp 169–282.
- (4) Fischer, R. C.; Power, P. P. *Chem. Rev.* **2010**, *110*, 3877–3923.
- (5) Mizuhata, Y.; Sasamori, T.; Tokitoh, N. *Chem. Rev.* **2009**, *109*, 3479–3511.
- (6) Lee, V. Y.; Fukawa, T.; Nakamoto, M.; Sekiguchi, A.; Tumanskii, B. L.; Karni, M.; Apeloig, Y. *J. Am. Chem. Soc.* **2006**, *128*, 11643–11651.
- (7) Klinkhammer, K. W.; Schwarz, W. *Angew. Chem., Int. Ed. Engl.* **1995**, *34*, 1334–1336.
- (8) Klinkhammer, K. *Polyhedron* **2002**, *21*, 587–598.
- (9) Arp, H.; Baumgartner, J.; Marschner, C.; Müller, T. *J. Am. Chem. Soc.* **2011**, *133*, 5632–5635.
- (10) Kayser, C.; Kickelbick, G.; Marschner, C. *Angew. Chem., Int. Ed.* **2002**, *41*, 989–992.
- (11) Fischer, R.; Frank, D.; Gaderbauer, W.; Kayser, C.; Mechtler, C.; Baumgartner, J.; Marschner, C. *Organometallics* **2003**, *22*, 3723–3731.
- (12) Welch, G. C.; Prieto, R.; Dureen, M. A.; Lough, A. J.; Labeodan, O. A.; Holtrichter-Rossmann, T.; Stephan, D. W. *Dalton Trans.* **2009**, 1559–1570.
- (13) Wrackmeyer, B.; Stader, C.; Horchler, K. J. *Magn. Reson.* **1989**, *83*, 601–607.
- (14) Fischer, R.; Konopa, T.; Baumgartner, J.; Marschner, C. *Organometallics* **2004**, *23*, 1899–1907.
- (15) Müller, T. *J. Organomet. Chem.* **2003**, *686*, 251–256.
- (16) Klett, J.; Klinkhammer, K. W.; Niemeyer, M. *Chem.—Eur. J.* **1999**, *5*, 2531–2536.
- (17) Eaborn, C.; Ganicz, T.; Hitchcock, P. B.; Smith, J. D.; Sözerli, S. E. *Organometallics* **1997**, *16*, 5621–5622.
- (18) Klinkhammer, K. Silyl-derivate der schweren Alkalimetalle in der Synthese niedervalenter Hauptgruppenelementverbindungen, habilitation thesis, Universität Stuttgart, 1998.
- (19) Mean value from  $\delta^{29}\text{Si} = -33$  and  $\delta^{29}\text{Si} = -37$  predicted for the two nonequivalent  $\alpha$ -Si-atoms in the optimized structure of plumbylene **6** at the GIAO/B3LYP/6-311+G(2d,p)(Si,C,H,def2TZVP(Pb))/M06-2X/A level of theory; see Supporting Information for further details.
- (20) The pyramidalization angle  $\beta$  is defined as the angle between the vector of the exocyclic E–Pb bond and the plane spanned by the Pb atom and the two adjacent Si atoms.
- (21) Pyykkö, P.; Atsumi, M. *Chem.—Eur. J.* **2009**, *15*, 12770–12779.
- (22) Mantina, M.; Chamberlin, A. C.; Valero, R.; Cramer, C. J.; Truhlar, D. G. *J. Phys. Chem. A* **2009**, *113*, 5806–5812.
- (23) Preut, H.; Huber, F. Z. *Anorg. Allg. Chem.* **1976**, *419*, 92–96.
- (24) Weidenbruch, M.; Kilian, H.; Peters, K.; Schneringer, H. G. V.; Marsmann, H. *Chem. Ber.* **1995**, *128*, 983–985.
- (25) Stabenow, F.; Saak, W.; Marsmann, H.; Weidenbruch, M. *J. Am. Chem. Soc.* **2003**, *125*, 10172–10173.
- (26) Stürmann, M.; Weidenbruch, M.; Klinkhammer, K. W.; Lissner, F.; Marsmann, H. *Organometallics* **1998**, *17*, 4425–4428.
- (27) Stürmann, M.; Saak, W.; Marsmann, H.; Weidenbruch, M. *Angew. Chem., Int. Ed.* **1999**, *38*, 187–189.
- (28) The Gaussian 09 program was used. Gaussian 09 Revision B. 01; Gaussian, Inc.: Wallingford, 2010.
- (29) For detailed description of the computations, see the Supporting Information.

(30) Pb(II)Si(IV) bonds in plumbylene 270–271 pm, see: Klinkhammer, K. In *The Chemistry of Organic Germanium, Tin and Lead Compounds Vol. 2*; Rappoport, Z., Ed.; John Wiley & Sons, Ltd.: 2002; pp 283–357.

(31) The donor–acceptor bond strengths or binding energies, BE, were computed using the computed total energy of the complex and subtracting the computed total energies of its constituent molecules. Therefore, a more negative BE means a stronger bond.

(32) For a detailed description of the NBO analyses with respect to the negative hyperconjugation, see Supporting Information.

(33) Entropy and solvation effects favor the dissociation of dimer **4** into the two constituent plumblyenes **6**. This is detailed and quantified in the Supporting Information (Figure S8). Therefore, the here reported BE for dimer **4** is in agreement with detection of the monomer **6** in toluene solution.

(34) Computed for charges of opposite sign of 0.24 au (resulting from the NBO analysis) in a distance of 309.9 pm (calculated  $d(\text{Pb}(1)\text{Pb}(2))$  in dimer **4**).

(35) Wiberg, N.; Schuster, H.; Simon, A.; Peters, K. *Angew. Chem.* **1986**, *98*, 100–101.

(36) (a) Masters (née Hinchley), S. L.; Grassie, D. A.; Robertson, H. E.; Hölbling, M.; Hassler, K. *Chem. Commun.* **2007**, 2618–2620. (b) Bock, H.; Solouki, B. In *The Chemistry of Organic Silicon Compounds*, Vol. 3; Apeloig, Y., Rappoport, Z., Eds.; Wiley: Chichester, 2001; p 187.

(37) Sieffert, N.; Bühl, M. *Inorg. Chem.* **2009**, *48*, 4622–4624.

(38) (a) Schreiner, P. R.; Chernish, L. V.; Gunchenko, P. A.; Tikhonchuk, E. Y.; Hausmann, H.; Serafin, M.; Schlecht, S.; Dahl, J. E. P.; Carlson, R. M. K.; Fokin, A. A. *Nature* **2011**, *477*, 308–311. (b) Grimme, S.; Schreiner, P. R. *Angew. Chem., Int. Ed.* **2011**, *50*, 12639–12642.

(39) Zhao, Y.; Truhlar, D. G. *Theor. Chem. Acc.* **2007**, *120*, 215–241.

(40) Adapted from Goethe, J. W. “Faust”, J. G. Cotta’schen Buchhandlung Tübingen 1808, translated by Priest, G. M. Princeton University, 1932.

(41) Takahashi, M.; Tsutsui, S.; Sakamoto, K.; Kira, M.; Müller, T.; Apeloig, Y. *J. Am. Chem. Soc.* **2000**, *123*, 347–348.

(42) Pangborn, A. B.; Giardello, M. A.; Grubbs, R. H.; Rosen, R. K.; Timmers, F. J. *Organometallics* **1996**, *15*, 1518–1520.

(43) Morris, G. A.; Freeman, R. *J. Am. Chem. Soc.* **1979**, *101*, 760–762.

(44) Helmer, B. J.; West, R. *Organometallics* **1982**, *1*, 877–879.

(45) SAINTPLUS: Software Reference Manual, Version 6.45: Bruker-AXS: Madison, WI, 1997–2003.

(46) Blessing, R. H. *Acta Crystallogr., Ser. A* **1995**, *51*, 33–38.

(47) SADABS: Version 2.1; Bruker-AXS: Madison, WI, 1998.

(48) Sheldrick, G. M. *Acta Crystallogr., Ser. A* **2008**, *64*, 112–122.

(49) Lancaster, S. Alkylation of boron trifluoride with pentafluorophenyl Grignard reagent; Tris(pentafluorophenyl)boron. <http://cssp.chemspider.com/215> (accessed Nov 21, 2011).